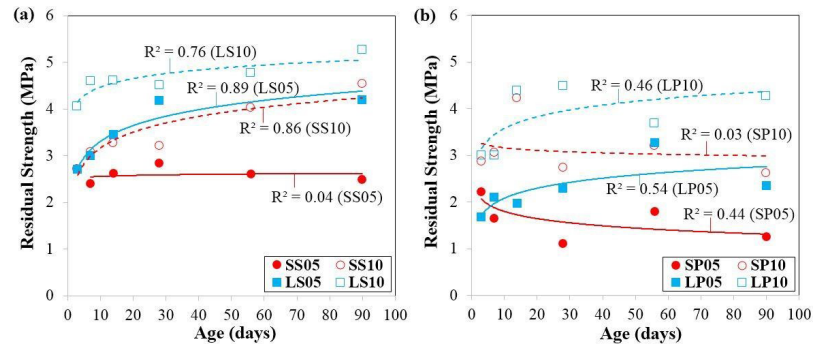


MOUNTAIN-PLAINS CONSORTIUM

MPC 18-353 | A. Bordelon and M. Kim

Early-Age Fiber-Reinforced Concrete Properties for Overlays



A University Transportation Center sponsored by the U.S. Department of Transportation serving the Mountain-Plains Region. Consortium members:

Colorado State University
North Dakota State University
South Dakota State University

University of Colorado Denver
University of Denver
University of Utah

Utah State University
University of Wyoming

**EARLY-AGE FIBER-REINFORCED CONCRETE
PROPERTIES FOR OVERLAYS**

Min Ook Kim, Ph.D.
Senior Research Scientist
Korea Institute of Ocean Science and Technology

Amanda Christine Bordelon, Ph.D., P.E.
Assistant Professor
Department of Engineering
Utah Valley University

July 2018

Acknowledgements

The authors would like to thank the Mountain-Plains Consortium Project 492; University of Utah Department of Civil Engineering; and Utah Department of Transportation for providing funding for this research. The authors thank the initial reviewers of this project idea for their useful feedback on the topic, as well as thank the academic supervisory committee of Dr. Chris P. Pantelides, Dr. Pedro Romero, Dr. Luis Ibarra, and Dr. Eunhye Kim for their valuable comments and suggestions.

Disclaimer

The contents of this report reflect the views of the authors, who are reasonable for the facts and the accuracy of the information presented. This document is disseminated under the sponsorship of the Department of Transportation, University Transportation Centers Program, in the interest of information exchange. The U.S. Government assumes no liability for the contents or use thereof.

NDSU does not discriminate in its programs and activities on the basis of age, color, gender expression/identity, genetic information, marital status, national origin, participation in lawful off-campus activity, physical or mental disability, pregnancy, public assistance status, race, religion, sex, sexual orientation, spousal relationship to current employee, or veteran status, as applicable. Direct inquiries to Vice Provost, Title IX/ADA Coordinator, Old Main 201, 701-231-7708, ndsuetoo@ndsuetoo.edu.

ABSTRACT

This study aims to investigate the age-dependent changes in flexural and fracture properties of fiber-reinforced concrete (FRC) used in the design of thin overlay pavements. Four different types of steel or polypropylene macro-fibers with different dimensions and different fiber volume contents (0%, 0.5%, and 1.0%) were selected and investigated. No significant changes in compressive strength, free drying shrinkage, coefficient of thermal expansion, and modulus of rupture versus age were identified. Steel FRCs were observed to have a constant or increased residual strength as a function of age while different types or contents of polypropylene FRCs showed varied trends in residual strength versus age. Fracture energy for all FRCs was observed to increase versus age. The residual strength ratio for all FRCs decreased as a function of age, but with only two replicates per age and FRC type, and values were highly variable so no trends were statistically verified at this time. A standard test age, namely 28 days, is recommended due to the changing residual strength ratio parameter used in thin FRC overlay design.

TABLE OF CONTENTS

1. INTRODUCTION	1
2. EXPERIMENTAL INVESTIGATION	4
2.1 Mixture Design and Test Variables	4
2.2 Test Specimens and Measurement Ages.....	5
2.3 Data Analysis.....	6
3. EXPERIMENTAL RESULTS AND DISCUSSION	9
3.1 Compressive Strength	9
3.2 Shrinkage	9
3.3 Coefficient of Thermal Expansion.....	10
3.4 Flexural Strength.....	11
3.5 Residual Strength and Residual Strength Ratio	15
3.6 Fracture Energy.....	20
4. CONCLUSIONS	22
5. REFERENCES	23

LIST OF TABLES

Table 2.1	Properties of Fibers	5
Table 2.2	Mix Proportions of Plain Concrete and FRC Mixtures.....	5
Table 3.1	Averaged First Crack Flexural Properties of Both Plain and FRC Specimens	12
Table 3.2	Averaged Post-Cracking Properties of FRC Specimens	14
Table 3.3	Averaged Residual Strength and Toughness of FRC Specimens (ASTM Method)	16
Table 3.4	Averaged Residual Strength Ratios, $R_{150ASTM}$ and $R_{150JSCE}$	18
Table 3.5	Averaged Wedge Splitting Fracture Energy of Plain and FRC Specimens	21

LIST OF FIGURES

Figure 1.1	Age-dependent changes in residual strength ratio for (a) SFRC and (b) PFRC (Bernard 2015).....	2
Figure 2.1	Selected fibers: (a) short steel (SS); (b) long steel (LS); (c) short polypropylene (SP); (d) long polypropylene (LP).....	4
Figure 2.2	Wedge splitting test configuration and photograph of setup.....	6
Figure 2.3	Typical load-deflection curves of FRC.....	7
Figure 3.1	Compressive strength versus age for (a): SFRC and (b): PFRC.....	9
Figure 3.2	Free drying shrinkage versus age for (a): SFRC and (b): PFRC.....	10
Figure 3.3	Coefficient of thermal expansion for different specimens.....	10
Figure 3.4	Load versus deflection of a FRC beam containing either (a) and (b) for SS10 or (c) and (d) for SP10. Plots show both the smaller deflection values (between 0 and 0.5 mm) and full deflection test range (between 0 and 4.0 mm).....	11
Figure 3.5	Modulus of rupture versus age for (a): SFRC and (b): PFRC.....	13
Figure 3.6	Residual strength versus age for (a): SFRC and (b): PFRC.....	17
Figure 3.7	Residual strength ratio versus age, (a) and (c) for SFRC and (b) and (d) for PFRC.....	19
Figure 3.8	Effects of fiber length, aspect ratio, volume fraction and material type on ASTM residual strength ratio.....	20
Figure 3.9	Fracture energy versus age for (a): SFRC and (b): PFRC.....	21

EXECUTIVE SUMMARY

Fiber-reinforced concrete (FRC) has been used for concrete pavement overlays for a few decades. It is well documented to improve performance over unreinforced plain concrete in the aspects related to crack initiation, and crack propagation. When selecting an appropriate fiber-reinforced concrete for the design of thin overlays, the flexural residual strength is the primary design criteria used. Other material parameters, such as slump, unit weight, air content, compressive strength, shrinkage, and coefficient of thermal expansion, are also commonly measured to determine consistency between mixtures and to be used in design software as the baseline material properties.

One major challenge with the FRC industry and use in pavements is that the test does not specify at what age these tests should be performed. It was hypothesized that the FRC properties change with age and that not having a specified age for the test to be performed would result in variable performance in the field. This research project measured four types of fibers mixed into the same basic matrix and tested fresh and hardened properties used in the field and in design for FRC from age three to 90 days. The results indicated that the age of testing does influence most material properties. The design specified flexural strength test for FRC was especially found to give statistically significant different material properties when tested for the same mixture at different ages. For consistency in future use of FRC for overlay pavements, it was recommended that a specified age be made. For practical purposes, the authors recommend an age of 28 days at this time.

1. INTRODUCTION

Fibers have been widely utilized as reinforcement in various concrete infrastructure, including concrete overlays (Carlswård 2006; Chanvillard et al. 1989), bridge decks (Krstulovic-Opara et al. 1995), high-rise buildings (Lu et al. 2013), and marine concrete structures (Hoff 1987; Mangat and Gurusamy 1987). Many experimental studies have been carried out to investigate how fibers added to concrete will improve toughness, cracking resistance, and interfacial bond (Banthia and Sheng 1996; Bayasi and Zeng 1993; Gopalaratnam et al. 1991; Jenq and Shah 1986; Kim and Bordelon 2015, 2016; Mobasher et al. 2014; Song et al. 2005; Wang et al. 1990; Ward and Li 1990). There are some existing testing procedures to evaluate the flexural performance of fiber-reinforced concrete (FRC), such as ASTM C1609 (ASTM C1609 2010), JSCE-SF 4 (Japan Society of Civil Engineers 1984), BS EN14651 (British Standards Institute 2005), and RILEM TC 162-TDF (RILEM TC 162-TDF 2003).

The design of FRC overlays utilizes a residual strength ratio (R_{150}), which is measured based on the post-cracking flexural stress carried by the FRC normalized by the flexural strength at first cracking (MOR). Reported FRC property measurements have been typically undertaken at 28 days. The 28-day strength is considered close to the material's final strength and generally accepted for the structural design of various concrete structures, including concrete overlays. However, the concrete strength does not stop increasing at 28 days, but for many months thereafter. As such, the residual strength ratio may in fact decrease with age since the flexural strength in the denominator is expected to increase. Alternatively, if the residual strength of the FRC correspondingly increases with age besides the flexural strength, the residual strength ratio can be consistent or increased as time goes by. In this regard, understanding the age-dependent FRC properties is crucial for predicting cracking or improving the design of FRC overlays.

Altoubat et al. (2008) proposed the following Eq. (1) to determine the effective modulus of rupture, MOR_{eff} for FRC overlay design.

$$MOR_{eff} = MOR(1 + R_{150}) \quad (1)$$

In Eq. (1), R_{150} is FRC residual strength ratio, which can be zero in plain concrete pavement design. The stress ratio used to for fatigue prediction of concrete pavements, SR_{total} , is estimated by dividing the total tensile stress from traffic and environment loading, σ_{total} , by MOR_{eff} as shown in Eq. (2) (Altoubat et al. 2008).

$$SR_{total} = \frac{\sigma_{total}}{MOR_{eff}} \quad (2)$$

In FRC overlay design, it is preferred that the MOR_{eff} increase with time to provide more resistance against continued traffic loads.

The fiber effect on compressive and flexural strengths has been investigated by past researchers (Bolat et al. 2014; Campione 2006; Chanh 2004; Fraternali et al. 2011; Hsie et al. 2008; Koo et al. 2014; Meddah and Bencheikh 2009; Ochi et al. 2007; Pereira De Oliveira and Castro-Gomes 2011; Ward and Li 1990). Among the previous studies, steel fiber-reinforced concrete (SFRC) at 1% to 2% fiber volume fraction has been claimed to increase compressive strength due to dowel-like resistance of the added fibers, which bridge internal defects in the event that failure is initiated (Bolat et al. 2014; Chanh 2004; Ward and Li 1990). On the other hand, some researchers pointed out that polypropylene fibers can reduce the compressive strength as a function of increasing fiber volume content (Campione 2006; Fraternali et al. 2011; Hsie et al. 2008; Ochi et al. 2007; Pereira De Oliveira and Castro-Gomes 2011). This reduction in compressive strength is speculated as due to compaction or mixing difficulties with high contents of the polypropylene fibers. In terms of flexural properties, polypropylene fiber-reinforced concrete (PFRC) has been found to improve the post-cracking flexural toughness of concrete without a significant influence on

the measured peak flexural strength compared with plain concrete (Koo et al. 2014; Meddah and Bencheikh 2009; Ochi et al. 2007; Pereira De Oliveira and Castro-Gomes 2011). Micro-FRC samples were noted to have a reduced free drying shrinkage as compared with macro-FRC and plain concrete (Soliman and Nehdi 2014). Researchers have found that the effect of macro-fibers on free drying shrinkage is negligible at low fiber volume contents (Grzybowski and Shah 1990; Malmberg and Skarendhal 1978). Yet, Zhang and Li (2001) reported steel macro-FRC at higher volume contents more than 1% of the time exhibited reduced free drying shrinkage compared with plain concrete. Another important parameter of concrete used in pavement design is the coefficient of thermal expansion (CTE). The CTE is presumed to be influenced by aggregate type and the quantity of coarse aggregate (Shin and Chung 2011). While it is not expected that the CTE changes with ages of less than 28 days (Buch et al. 2008; Won 2005), it, too, will be studied to determine if the CTE might change with the addition of fibers.

Some experimental studies have been carried out to investigate other age-dependent FRC properties (Bernard 2015; Bordelon 2007; Chan and Li 1997; Hodicky et al. 2013). An earlier study by Bernard (2015), which tested FRC at different ages, found that SFRC and PFRC exhibited a decreased or constant residual strength ratio between seven and 90 days, as represented in Figure 1.1. Bordelon (2007) also reported a reduction of residual strength ratio of PFRC between seven and 28 days. Conversely to flexural tests, a wedge-split fracture test by Hodicky et al. (2013) found that tensile strength and fracture energy of SFRC were both increased with age. On a microstructure level, the fiber-to-cement interfacial bond between 0.5 to 28 days, as determined from a pull-out test, was found by researchers to only increase within the first two days, but have no significant change from seven to 28 days (Chan and Li 1997).

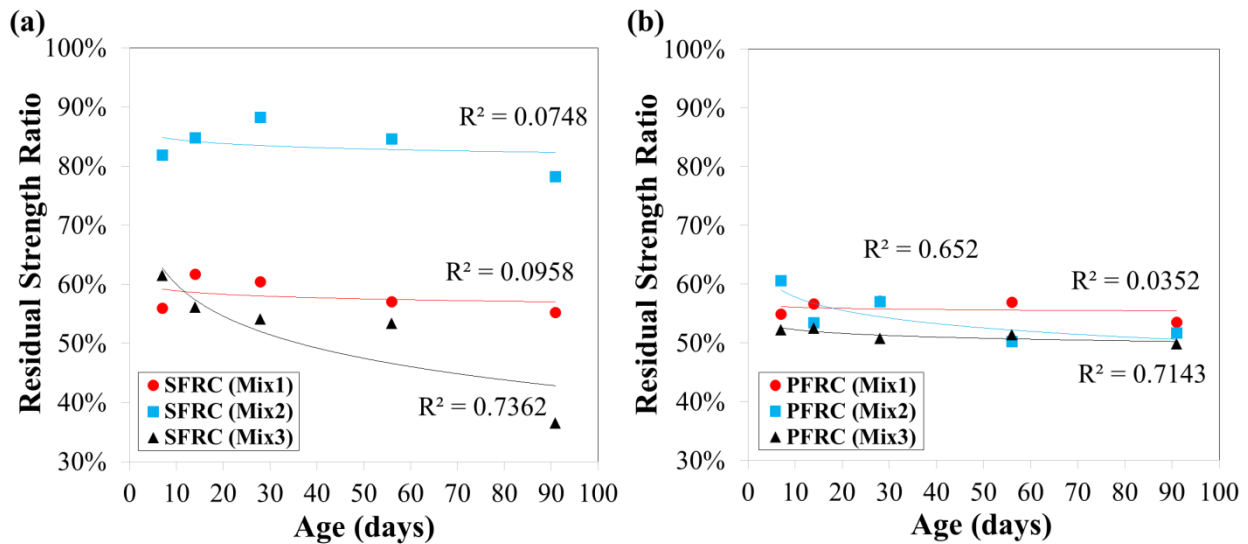


Figure 1.1 Age-dependent changes in residual strength ratio for (a) SFRC and (b) PFRC (Bernard 2015)

The objective of this study was to investigate the age-dependent changes in mechanical properties of FRC, which can be utilized for FRC overlay design. A standard flexural beam and wedge-splitting fracture test were conducted on FRC samples at ages between three and 90 days. The general concrete properties of compressive strength, free drying shrinkage, and coefficient of thermal expansion are not expected to change due to the fiber content, but were also tested for confirmation in this study.

While the residual strength ratio used in FRC overlay design is presumed to be measured at 28 days, the age-dependency of flexural and fracture properties of FRC have not been well integrated in test requirements. It is expected that FRC exhibits age-dependent changes in residual strength ratio, and thus it is critical for a pavement engineer to select the desired age of testing so that the residual strength ratio can be ultimately linked with the long-term performance of FRC overlays. Understanding age-dependent changes in residual strength or residual strength ratio can then provide engineers tips to determine optimum fiber type and volume content. For these reasons, an experimental program was set up and a comprehensive experimental campaign was conducted to investigate the effects of different fiber types and volume contents on age-dependent properties of FRC. The first crack load, second peak, or maximum peak load were measured, and both residual strength and residual strength ratio were calculated according to ASTM and JSCE methods.

2. EXPERIMENTAL INVESTIGATION

2.1 Mixture Design and Test Variables

Figure 2.1 and Table 2.1 show the selected fibers and material properties used in this study, respectively. All selected fibers are commonly used in concrete overlays or thin shell structures. The nomenclature for this paper labels the fibers as short steel hooked (SS), long steel hooked (LS), short polypropylene (SP), and long polypropylene (LP) based on the comparative fiber length and fiber type. This study focuses more on the age-dependent changes in flexural or fracture properties of FRCs, rather than the effect of fiber length or fiber type. For example, the direct comparison between the two PFRCs can be meaningless since these two polypropylene fibers have very different geometrical and mechanical properties (e.g., tensile strength and elastic modulus) as listed in Table 2.1. Table 2.2 shows the concrete mixture proportions utilized in this study designed for 1 m³ of total plain concrete volume. All FRC specimens were cast with the mass proportions listed in Table 2.2 such that the volumetric fraction of fibers was either 0.5% or 1.0% of the total FRC mixture. All mixtures contained the same dosage of polycarboxylate high range water reducer (HRWR).

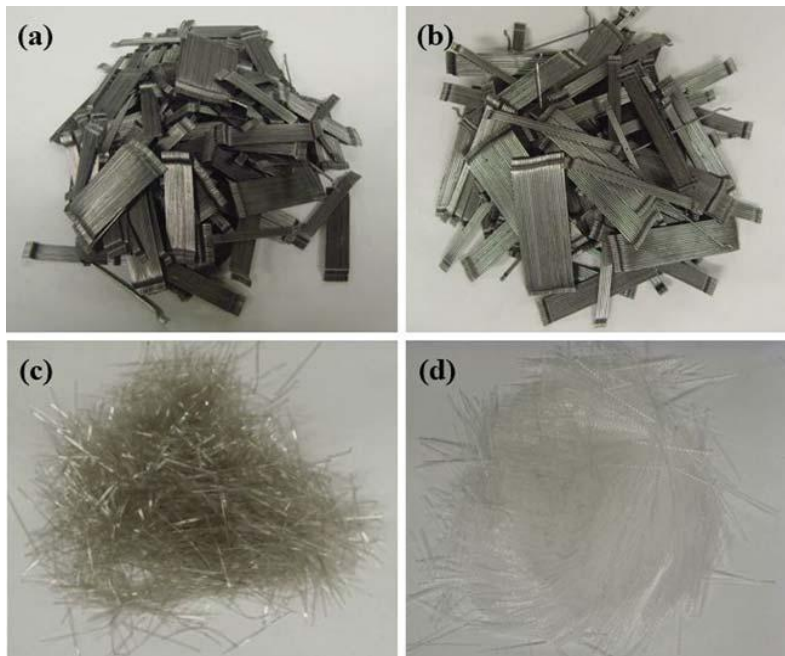


Figure 2.1 Selected fibers: (a) short steel (SS); (b) long steel (LS); (c) short polypropylene (SP); (d) long polypropylene (LP).

Table 2.1 Properties of Fibers

Fiber Type	Material	Cross Section	Length (mm)	Diameter (mm)	Thickness (mm)	Width (mm)	Aspect Ratio	Tensile Strength (MPa)	Elastic Modulus (GPa)
SS	Short steel hooked	Circular	35	0.55	-	-	65	1345	210
LS	Long steel hooked	Circular	60	0.90	-	-	65	1160	210
SP	Short polypropylene	Rectangular	40	-	0.11	1.40	90	620	9.5
LP	Long polypropylene	Rectangular	50	-	0.40	1.20	75	550	7.0

Table 2.2 Mix Proportions of Plain Concrete and FRC Mixtures

Specimen	Water	Cement	Fly Ash	Coarse Aggregate	Fine Aggregate	Super Plasticizer	Air Entraining Admixture	Fiber
	kg/m ³	mL/m ³	mL/m ³	kg/m ³				
Plain	188	294	125	1053	856	1025	108	0
SS05	188	294	125	1053	856	1025	108	40
SS10	188	294	125	1053	856	1025	108	79
LS05	188	294	125	1053	856	1025	108	40
LS10	188	294	125	1053	856	1025	108	79
SP05	188	294	125	1053	856	1025	108	4.5
SP10	188	294	125	1053	856	1025	108	9
LP05	188	294	125	1053	856	1025	108	4.5
LP10	188	294	125	1053	856	1025	108	9

All fibers were dispersed by hand and mixed for two minutes into a rotary drum mixer after the plain concrete was mixed. The FRC was placed in the molds using a hand scoop and vibrated using a vibrating table. FRC specimens were demolded after 24 hours of casting and moist cured at a temperature around 23°C and 98% relative humidity until the age of testing. Specimens for free drying shrinkage were placed in a controlled temperature and humidity chamber at 23°C and 50% relative humidity after demolding.

2.2 Test Specimens and Measurement Ages

The compressive strength of FRC was determined using an average of three standard 100 × 200 mm cylinder specimens according to the ASTM C39 (2005). The flexural strength of FRC was determined using an average of two standard 150 × 150 × 533 mm beams with a span of 450 mm and a constant loading rate of 0.10 mm/min according to the ASTM C1609 (2010). A mounted deflection frame and a calculated average deflection from two LVDTs were used to estimate the mid-span deflection of the flexure beams. All strengths were measured from samples at the ages of 3, 7, 14, 28, 56, and 90 days.

Fracture properties of the FRC were determined using an average of two cube specimens of 150 × 150 × 150 mm with a 50 mm of initial pre-formed notch length as shown in Figure 2.2. Cube specimens were tested according to a wedge-splitting tensile test method (Brühwiler and Wittmann 1990). The splitting force was applied with a wedge of 9.1 degree total angle through a roller assembly at a constant vertical deflection rate of 1.0 mm/min. The crack opening displacement (COD) was recorded from two LVDTs mounted to the sides of the specimen near the initial notch tip. Fracture properties were measured at the ages of 7, 28, and 90 days.

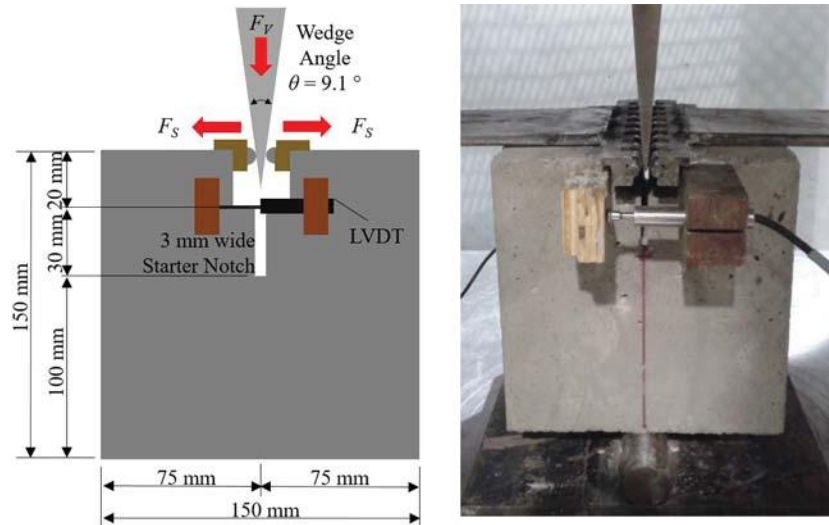


Figure 2.2 Wedge splitting test configuration and photograph of setup

The CTE was recorded according to AASHTO T336 (American Association of State Highway and Transportation Officials 2011) and only one sample at 1.0% of volume of each fiber type was measured at one age between three and 36 days. The free drying shrinkage of the FRC was determined using an average of three standard $75 \times 75 \times 286$ mm prismatic specimens by measuring the length change according to ASTM C157 (2008).

2.3 Data Analysis

The properties from the flexural beam test were analyzed according to ASTM C1609-10 (2010), JSCE-SF4 (Japan Society of Civil Engineers 1984), and Naaman and Reinhardt (2006). Figure 2.3 shows a typical flexural load versus deflection curve of FRC. The first crack load (P_1) is defined as the first point on the load-deflection curve when the slope is zero and the concrete initially cracks. The reported modulus of rupture is determined as the flexural strength from this first cracking. In some deflection-hardening samples, the sample continues to carry load to a higher value; in this case the ultimate load is defined as P_{max} (Kim et al. 2008; Mobasher et al. 2014; Naaman and Reinhardt 2006). Naaman and Reinhardt (2006) suggested recording the secondary peak load for deflection-softening samples, in this case labelled P_2 . The recorded load values are summarized as follows:

1. P_1 : First crack load; either used for *MOR* with deflection-softening, or called the Limit of Proportionality with deflection-hardening
2. P_{max} : Maximum peak load for deflection-hardening
3. P_2 : Second peak load for deflection-softening
4. $P_{L/150}$: The load reading for when the mid-span deflection reaches 1/150 (3 mm in this study) of the span.

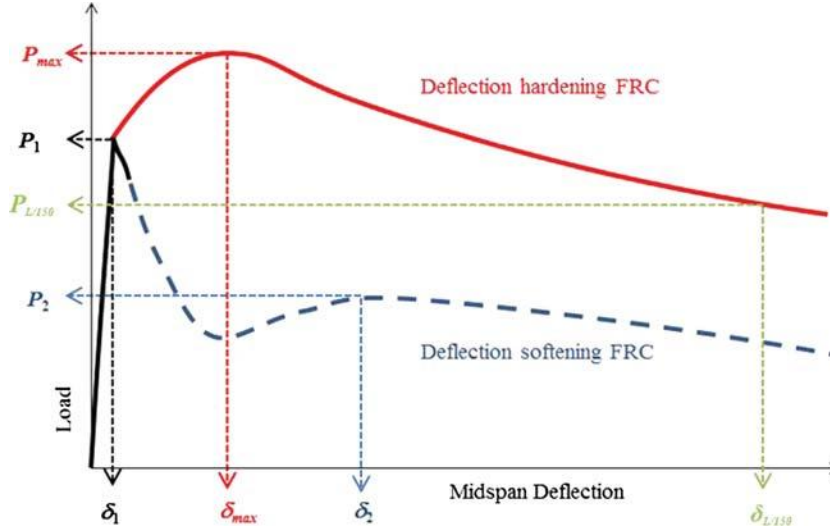


Figure 2.3 Typical load-deflection curves of FRC

The stresses are then calculated at the first crack, and maximum deflection-hardening peak, or deflection-softening second peak, based on Eqs. (3), (4), or (5), respectively.

$$f_1 = P_1 \cdot \frac{L}{bh^2} \quad (3)$$

$$f_{max} = P_{max} \cdot \frac{L}{bh^2} \quad (4)$$

$$f_2 = P_2 \cdot \frac{L}{bh^2} \quad (5)$$

where L is the span length ($=450$ mm), b is the width of specimen ($=150$ mm), and h is the height of specimen ($=150$ mm). According to the ASTM C1609-10 standard (ASTM C1609 2010), the residual stress, $f_{L/150}^{ASTM}$, and residual stress ratio, R_{150}^{ASTM} , can be calculated using Eqs. (6) and (7) shown below.

$$f_{L/150}^{ASTM} = P_{L/150} \cdot \frac{L}{bh^2} \quad (6)$$

$$R_{150}^{ASTM} = \frac{f_{L/150}^{ASTM}}{f_1} \times 100 \quad (7)$$

The JSCE-SF4 standard (Japan Society of Civil Engineers 1984) calculates the residual strength, $f_{L/150}^{JSCE}$, and residual strength ratio, R_{150}^{JSCE} , both based on the toughness as shown in Eqs. (8), (9), and (10), respectively.

$$T_{L/150} = \text{area}(P \cdot \delta)_0^{L/150} \quad (8)$$

$$f_{L/150}^{JSCE} = \frac{T_{L/150}}{L/150} \cdot \frac{L}{bh^2} \quad (9)$$

$$R_{150}^{JSCE} = \frac{f_{L/150}^{JSCE}}{f_1} \times 100 \quad (10)$$

where $T_{L/150}$ is the area under load-deflection curve between 0 and $L/150$ (=3 mm) of deflection. To analyze the results of wedge-splitting test, the splitting force, F_S , and a cut-off fracture energy $G_{FRC, 2.5 mm}$ were calculated using Eqs. (11) and (12).

$$F_S = \frac{F_V}{2 \tan\left(\frac{\theta}{2}\right)} \quad (11)$$

$$G_{FRC, 2.5 mm} = \frac{area(F_S \cdot COD)_0^{2.5}}{A} \quad (12)$$

where F_V is the vertical force applied through the wedge; θ is the total wedge angle; *area* is the sum of the area under the F_S versus average COD curve between 0 and 2.5 mm of averaged COD values, A is the area of the fracture path (=15000 mm²).

3. EXPERIMENTAL RESULTS AND DISCUSSION

3.1 Compressive Strength

Figure 3.1 (a) and (b) shows the measured compressive strength versus age for plain concrete and each FRC, respectively. A statistical p-value was calculated based first on dividing the individual sample property at each age relative to the average value of plain concrete samples at that age. The calculated p-values are also displayed in each figure for the better comparison between plain and FRCs. P-values less than 0.05, as found for most FRC samples, indicate that the compressive strengths are statistically different. In general, the SFRCs appear to have similar or slightly reduced compressive strengths, while the PFRCs all showed reduced compressive strengths compared with that of plain concrete. This might be due to compaction or mixing difficulties with high contents of the polypropylene fibers. Also, the effect of increased fiber volume content was not found to be significant. Although the strengths may be reduced with the addition of fibers, the compressive strength increase with age rate was not found to be different for FRC than plain concrete.

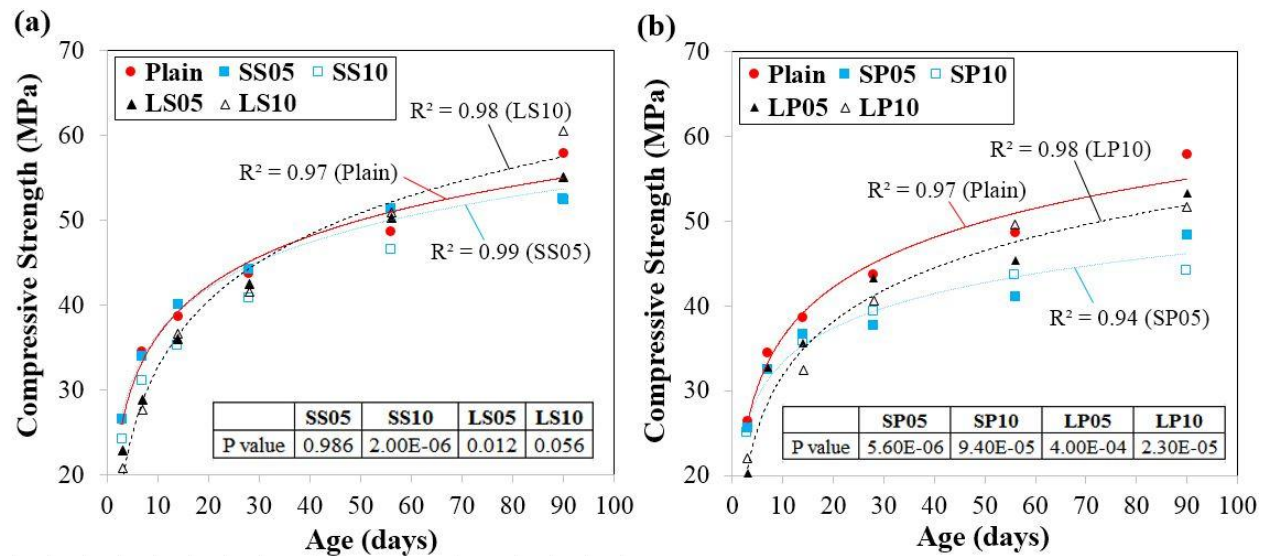


Figure 3.4 Compressive strength versus age for (a): SFRC and (b): PFRC

3.2 Shrinkage

Figure 3.2 (a) and (b) shows the measured free drying shrinkage from three to 90 days. The addition of fibers was confirmed to not substantially change (with most p-values greater than 0.05) the free drying shrinkage regardless of fiber type and content. This finding of insignificant influence from fibers on shrinkage is similar to what other researchers have described for similar fiber volume contents of 1.0% or less (Grzybowski and Shah 1990; Malmberg and Skarendhal 1978).

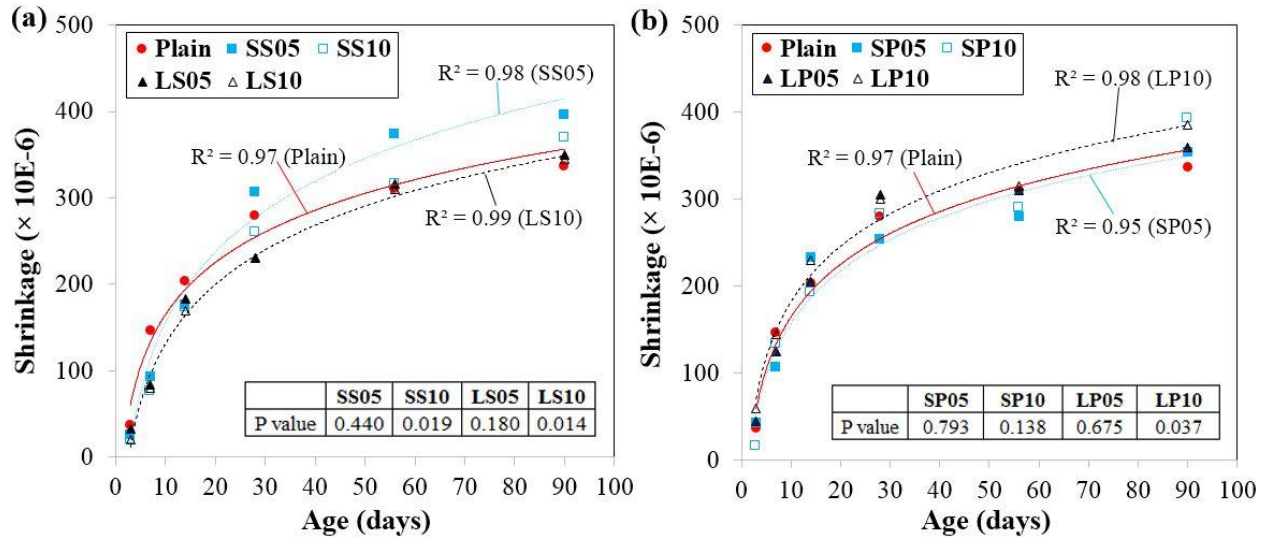


Figure 3.5 Free drying shrinkage versus age for (a): SFRC and (b): PFRC

3.3 Coefficient of Thermal Expansion

The coefficient of thermal expansion of one cylinder sample for mixtures at 1% volume fraction was measured. The CTE value of plain concrete was also measured to be $10.9 \times 10^{-6}/^{\circ}\text{C}$. Compared with the CTE value of plain concrete, SS10, SP10, and LP10 all had similar values of CTE. In more detail, these FRC CTE values were $11.0 \times 10^{-6}/^{\circ}\text{C}$, $11.3 \times 10^{-6}/^{\circ}\text{C}$, $11.1 \times 10^{-6}/^{\circ}\text{C}$, respectively, as seen in Figure 3.3. No sample was tested for LS10 at this time. Furthermore, no statistical analysis was carried out on CTE since there was only one sample of each mixture tested. Yet even with the limited sample data, the CTE appeared to exhibit negligible influence for a 1.0% volume fraction of fiber addition to the concrete.

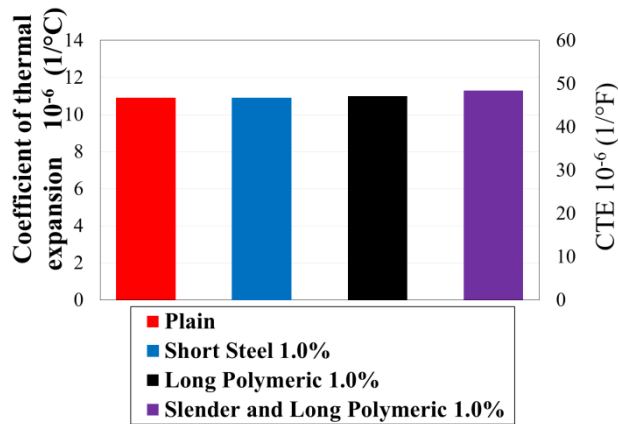


Figure 3.6 Coefficient of thermal expansion for different specimens

3.4 Flexural Strength

Figure 3.4 (a)-(d) shows representative load-deflection curves for SS10 and SP10 specimens. During the test, SS10, LS05, and LS10 underwent deflection-hardening responses after reaching the first crack load, while SS05 and all PFRCs exhibited deflection-softening responses. Table 3.1 lists the averaged first crack load, stress, and corresponding deflection for plain concrete and FRC specimens at each tested age. As shown in Figure 3.5, the first cracking modulus of rupture for all test specimens continuously increased between three and 90 days. There was no proven difference between plain concrete and FRCs for first cracking flexural strength, with most p-values greater than 0.05, except the set of 0.5% volume fraction of long SFRC samples appeared to be statistically higher than plain concrete. Overall, fibers are not expected to increase the flexural strength itself, but the post-cracking strength. If the highest or overall maximum flexural stress value was selected to describe the *MOR* in pavement design instead of the first-cracking stress, it is expected that the deflection-hardening samples clearly would have a statistically greater value compared with that of plain concrete. Among deflection-softening samples, no clear trend can be seen between the age and secondary peak stress. Table 3.2 shows the averaged maximum or secondary peak load, stress, and corresponding deflection for FRC specimens.

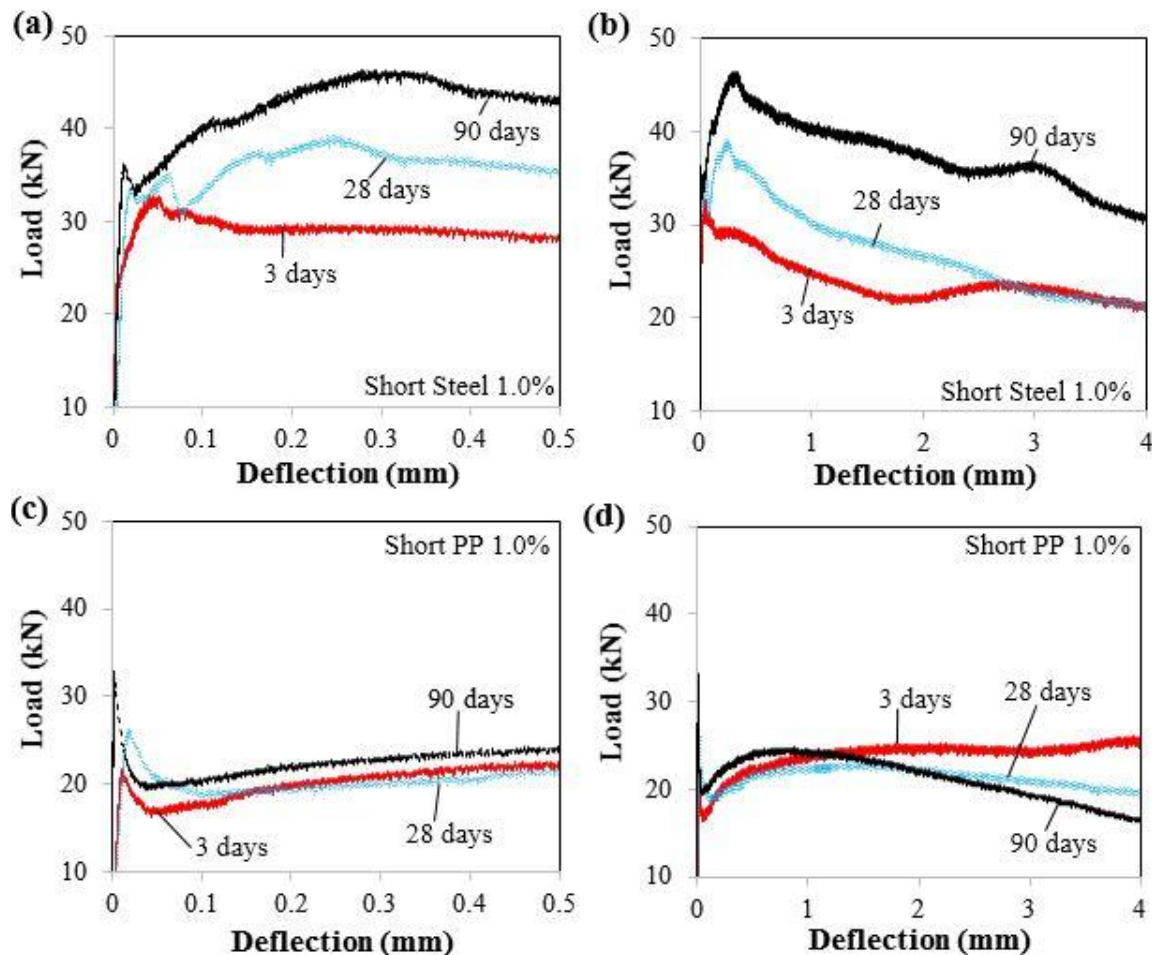


Figure 3.7 Load versus deflection of an FRC beam containing either (a) and (b) for SS10 or (c) and (d) for SP10. Plots show both the smaller deflection values (between 0 and 0.5 mm) and full deflection test range (between 0 and 4.0 mm).

Table 3.3 Averaged First Crack Flexural Properties of Both Plain and FRC Specimens

Specimen	Age (days)	3	7	14	28	56	90
Plain	P_1^a (N)	20,550	22,820	25,730	30,620	40,000	37,620
	f_1^b (MPa)	2.74	3.04	3.43	4.08	5.33	5.02
	δ_l^c (mm)	1.40E-02	2.00E-02	1.10E-02	6.00E-03	1.80E-02	8.00E-03
SS05	P_1 (N)	–	23,638	27,615	31,600	34,020	37,276
	f_1 (MPa)		3.15	3.68	4.21	4.54	4.97
	δ_l (mm)		3.00E-03	1.30E-02	1.00E-03	3.50E-02	4.20E-02
SS10	P_1 (N)	23,689	25,175	28,505	36,075	36,484	38,911
	f_1 (MPa)	3.16	3.36	3.8	4.81	4.87	5.19
	δ_l (mm)	6.00E-03	4.00E-03	1.40E-02	3.70E-02	1.40E-02	1.60E-02
LS05	P_1 (N)	23,402	23,304	29,051	33,295	–	49,086
	f_1 (MPa)	3.12	3.11	3.87	4.44		6.54
	δ_l (mm)	1.10E-02	7.00E-03	5.00E-03	3.00E-03		1.40E-02
LS10	P_1 (N)	24,312	26,723	24,988	31,087	36,609	44,222
	f_1 (MPa)	3.24	3.56	3.34	4.15	4.88	5.9
	δ_l (mm)	9.00E-03	1.00E-03	4.00E-03	2.00E-03	3.00E-03	1.40E-02
SP05	P_1 (N)	19,225	24,536	33,059	29,042	30,377	35,003
	f_1 (MPa)	2.56	3.27	4.41	3.87	4.05	4.67
	δ_l (mm)	6.00E-03	9.00E-03	8.00E-03	7.00E-03	4.00E-03	7.00E-03
SP10	P_1 (N)	19,613	26,761	29,523	26,623	30,740	32,810
	f_1 (MPa)	2.62	3.57	3.94	3.55	4.1	4.38
	δ_l (mm)	7.00E-03	1.20E-02	2.20E-02	1.00E-02	2.00E-03	3.00E-03
LP05	P_1 (N)	20,764	26,743	25,382	32,557	31,040	38,241
	f_1 (MPa)	2.77	3.57	3.38	4.34	4.14	5.1
	δ_l (mm)	1.10E-02	6.00E-03	6.00E-03	7.00E-03	2.00E-03	1.60E-02
LP10	P_1 (N)	24,370	23,033	28,066	31,569	32,917	40,830
	f_1 (MPa)	3.25	3.07	3.74	4.21	4.39	5.44
	δ_l (mm)	1.20E-02	1.00E-02	1.20E-02	7.00E-03	5.00E-03	6.00E-03

a First cracking load P_1

b First cracking stress f_1

c First cracking deflection δ_l

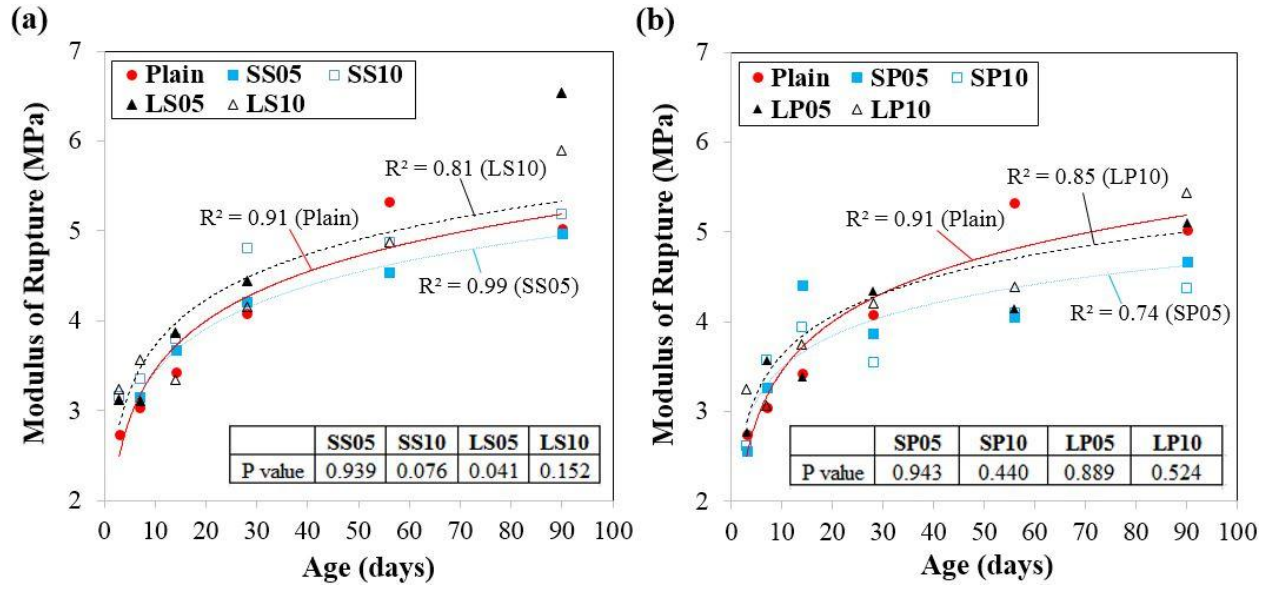


Figure 3.8 Modulus of rupture versus age for (a): SFRC and (b): PFRC

Table 3.4 Averaged Post-Cracking Properties of FRC Specimens

Specimen	Age (days)	3	7	14	28	56	90
SS05 (DS ^a)	P_2 (N)	–	23,153	28,744	35,639	26,485	25,777
	f_2 (MPa)		3.09	3.83	4.75	3.53	3.44
	δ_2 (mm)		4.80E-01	2.50E-01	2.30E-01	4.50E-01	4.10E-01
SS10 (DH ^b)	P_{max} (N)	35,586	36,921	36,544	43,943	50,974	51,573
	f_{max} (MPa)	4.74	4.92	4.87	5.86	6.8	6.88
	δ_{max} (mm)	1.70E-01	2.60E-01	2.30E-01	3.60E-01	2.50E-01	2.50E-01
LS05 (DH ^b)	P_{max} (N)	26,276	29,732	28,406	37,373	–	34,572
	f_{max} (MPa)	3.5	3.96	3.79	4.85		4.61
	δ_{max} (mm)	3.50E-01	7.90E-01	1.50E+00	4.80E-01		3.61E+00
LS10 (DH ^b)	P_{max} (N)	39,329	41,693	42,818	49,929	61,715	56,324
	f_{max} (MPa)	5.24	5.56	5.71	6.66	8.23	7.51
	δ_{max} (mm)	5.70E-01	1.80E+00	5.10E-01	6.50E-01	5.00E-01	2.90E-01
SP05 (DS ^a)	P_2 (N)	17,028	13,434	16,378	9386	13,923	12,032
	f_2 (MPa)	2.27	1.79	2.18	1.25	1.86	1.6
	δ_2 (mm)	3.00E+00	2.31E+00	9.40E-01	1.31E+00	2.68E+00	3.90E-01
SP10 (DS ^a)	P_2 (N)	22,575	26,029	32,005	21,734	27,419	23,554
	f_2 (MPa)	3.01	3.47	4.27	2.9	3.66	3.14
	δ_2 (mm)	3.57E+00	2.13E+00	2.74E+00	1.51E+00	2.32E+00	8.10E-01
LP05 (DS ^a)	P_2 (N)	13,785	18,322	15,195	17,989	26,040	17,922
	f_2 (MPa)	1.84	2.44	2.03	2.4	3.47	2.39
	δ_2 (mm)	2.70E+00	3.70E+00	3.58E+00	2.40E+00	3.52E+00	2.61E+00
LP10 (DS ^a)	P_2 (N)	25,844	24,817	37,327	34,928	30,397	36,578
	f_2 (MPa)	3.45	3.31	4.98	4.66	4.06	4.88
	δ_2 (mm)	9.30E-01	2.62E+00	2.41E+00	2.20E+00	2.41E+00	4.11E+00

^a Deflection-softening (DS): secondary peak load, P_2 , stress, f_2 , and deflection, δ_2 .

^b Deflection-hardening (DH): maximum peak load, P_{max} stress, f_{max} , and deflection, δ_{max} .

A closer look at the measured property values from Table 3.2 reveals that the deflection-hardening responses exhibited by SS10, LS05, and LS10 all were observed to have an increased f_{max} as a function of age, while deflection-softening responses of SS05 and all PFRCs did not show any trends for f_2 versus age. The effects of fiber volume fraction, fiber length, and fiber aspect ratio on measured f_{max} or f_2 were also summarized. The post-cracking stresses f_{max} or f_2 for all FRCs increased as fiber volume fraction or fiber length increased, as was expected based on previous research literature. Those trends are reasonable because increased effective bonding area with more fibers or longer fibers improve both flexural performance and cracking resistance. Uniquely, PFRCs showed a decrease in the f_2 as the aspect ratio increased. It is expected that the higher mechanical friction due to the embossed texture of the longer polypropylene fibers in comparison with the smooth surface of the shorter polypropylene fibers may also create a higher pull-out resistance.

3.5 Residual Strength and Residual Strength Ratio

In addition to MOR , the post-cracking residual strength is an important design parameter for thin FRC overlays. Regardless of when a pavement would crack as a function of the MOR , a constant residual strength f_{150} would indicate that a cracked overlay is still fundamentally resistant to the loading despite a reduced R_{150} value from the increased MOR . In this regard, constant or increased residual strengths versus age would be expected for an FRC mixture, regardless of the use of the residual strength ratio in the current design methodology. Table 3.3 shows the averaged residual strength $f_{L/150}^{ASTM}$ and toughness $T_{L/150}$ for each FRC. Figure 3.6 (a) and (b) illustrates the age-dependent changes in residual strength for SFRC and PFRC, respectively. The deflection-hardening samples (namely, SS10, LS05, and LS10) all were observed to have an increased $f_{L/150}^{ASTM}$ and $T_{L/150}$ as a function of age, while all deflection-softening samples did not show any trends (low R^2 values for a logarithmic fit) in $f_{L/150}^{ASTM}$ or $T_{L/150}$ versus age. Increased residual strengths were expected based on previous research by Bernard (2015), who reported increased residual strengths between three and 90 days for both SFRC and PFRC. The lack of trend found among deflection softening samples may be due to different fiber types, mixing, or casting procedures than Bernard's, or potentially due to high variability from a low number of replicate specimens tested for this study. The important finding from the results observed in Figure 3.6 (a) is that SFRCs overall do show a constant or increased residual strength versus age.

Table 3.5 Averaged Residual Strength and Toughness of FRC Specimens (ASTM Method)

Specimen	Age (days)	3	7	14	28	56	90
SS05	P_{L150} (N)	–	17,971	19,652	21,191	19,586	18,576
	f_{L150} (MPa)		2.4	2.62	2.83	2.61	2.48
	T_{L150} (Nm)		59.227	67.788	79.638	62.696	60.164
SS10	P_{L150} (N)	20,331	23,053	24,456	24,074	30,155	33,958
	f_{L150} (MPa)	2.71	3.08	3.26	3.21	4.03	4.53
	T_{L150} (Nm)	77.858	85.158	89.935	91.804	114.739	125.092
LS05	P_{L150} (N)	20,315	22,432	25,902	31,315	–	31,396
	f_{L150} (MPa)	2.71	2.99	3.45	4.18		4.19
	T_{L150} (Nm)	68.126	77.998	78.638	98.345		92.482
LS10	P_{L150} (N)	30,397	34,525	34,565	48,797	35,731	39,445
	f_{L150} (MPa)	4.06	4.6	4.61	6.51	4.77	5.26
	T_{L150} (Nm)	104.467	106.512	112.842	136.407	133.247	145.511
SP05	P_{L150} (N)	16,672	12,299	14,786	8265	13,385	9350
	f_{L150} (MPa)	2.22	1.64	1.97	1.1	1.79	1.25
	T_{L150} (Nm)	39.455	35.196	47.445	26.854	32.902	32.483
SP10	P_{L150} (N)	21,498	22,875	31,598	20,442	23,967	19,632
	f_{L150} (MPa)	2.87	3.05	4.22	2.73	3.2	2.62
	T_{L150} (Nm)	58.504	67.451	80.962	61.379	68.162	64.972
LP05	P_{L150} (N)	12,620	15,747	14,777	17,175	24,519	17,522
	f_{L150} (MPa)	1.68	2.1	1.97	2.29	3.27	2.34
	T_{L150} (Nm)	36.323	38.733	40.058	44.91	56.791	51.387
LP10	P_{L150} (N)	22,395	22,488	32,910	33,639	27,557	31,959
	f_{L150} (MPa)	2.99	3	4.39	4.49	3.68	4.26
	T_{L150} (Nm)	70.631	62.28	94.861	89.131	75.629	86.091

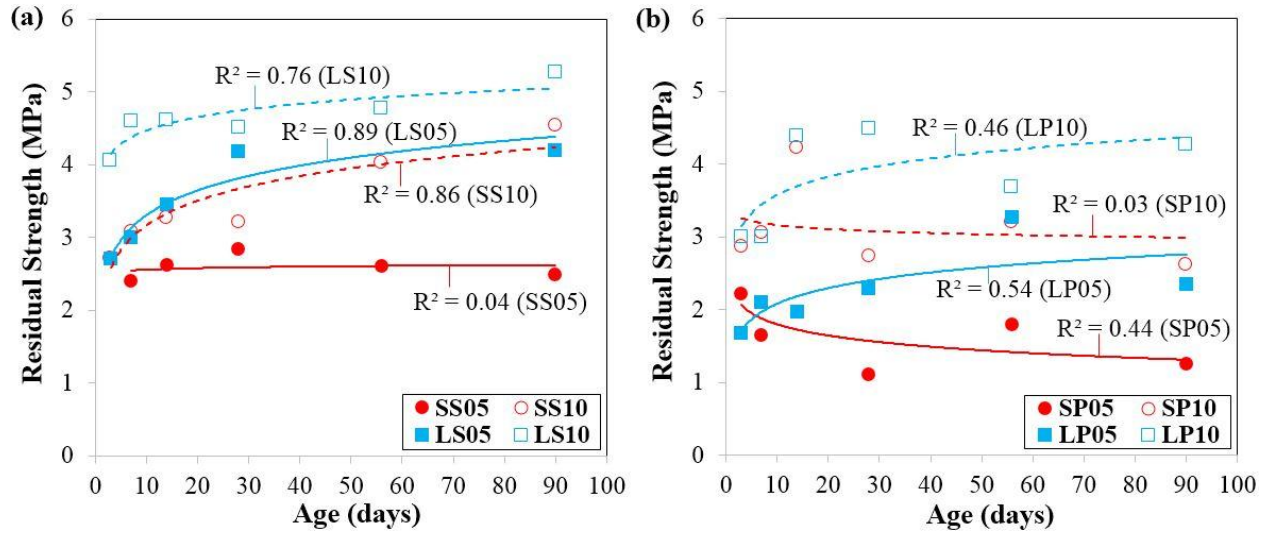


Figure 3.9 Residual strength versus age for (a): SFRC and (b): PFRC

Table 3.4 shows the calculated averaged residual strength ratios according to ASTM and JSCE. The R_{150} from two different standards showed similar values and correlation with age as expected. In Figure 3.7, R_{150}^{ASTM} and R_{150}^{JSCE} both illustrates a potential logarithmic fit for the different fiber types in relative residual capacity to carry load after failure if cracking occurs at various ages. Although the draw trend lines may indicate clear relationships, the calculated R^2 values for these trends is extremely low, indicating high variability or a poor fit. The proposed trend suggests that SFRCs and PFRCs exhibit a decreased R_{150} as a function of age. For example, based on the average R_{150} calculations for ages three versus 90 days, the SP05 and SP10, respectively, showed a 70% and 45% reduction in residual strength ratio. Importantly, the calculated ratio values for both SFRCs and PFRCs were highly variable, and no trend could be determined at this time. The high variability is similar to the result reported by other researchers, indicating that even with seven replicates, such as was reported and shown in Fig 1.1 (Bernard 2015), a high variability and low R^2 values are common with FRC test results.

Table 3.6 Averaged Residual Strength Ratios, R_{150}^{ASTM} and R_{150}^{JSCE}

Specimen	Age (days)	3	7	14	28	56	90
SS05	R_{150}^{ASTM}	-	76.2	57.7	67.2	70.9	49.9
	R_{150}^{JSCE}		83.6	66.4	84.1	75.7	53.7
SS10	R_{150}^{ASTM}	85.8	91.7	85.8	66.7	82.8	87.9
	R_{150}^{JSCE}	109.5	112.6	105.2	84.8	104.7	107.2
LS05	R_{150}^{ASTM}	86.9	96.1	89.1	94.1	-	64.1
	R_{150}^{JSCE}	97	111.5	90.3	98.4		62.8
LS10	R_{150}^{ASTM}	125.3	129.2	138	156.9	97.7	89
	R_{150}^{JSCE}	143.3	133	150.2	146.1	121.4	110.1
SP05	R_{150}^{ASTM}	86.7	50.2	44.7	28.4	44.2	26.8
	R_{150}^{JSCE}	68.5	47.8	47.8	30.8	36.1	30.9
SP10	R_{150}^{ASTM}	109.5	85.4	107.1	76.9	78	59.8
	R_{150}^{JSCE}	99.2	84	91.3	76.8	73.9	65.9
LP05	R_{150}^{ASTM}	60.6	58.8	58.3	52.8	79	45.9
	R_{150}^{JSCE}	58.3	48.2	52.7	46	61	44.8
LP10	R_{150}^{ASTM}	92	97.7	117.4	106.7	83.8	78.3
	R_{150}^{JSCE}	96.6	90.2	112.7	94.1	76.6	70.3

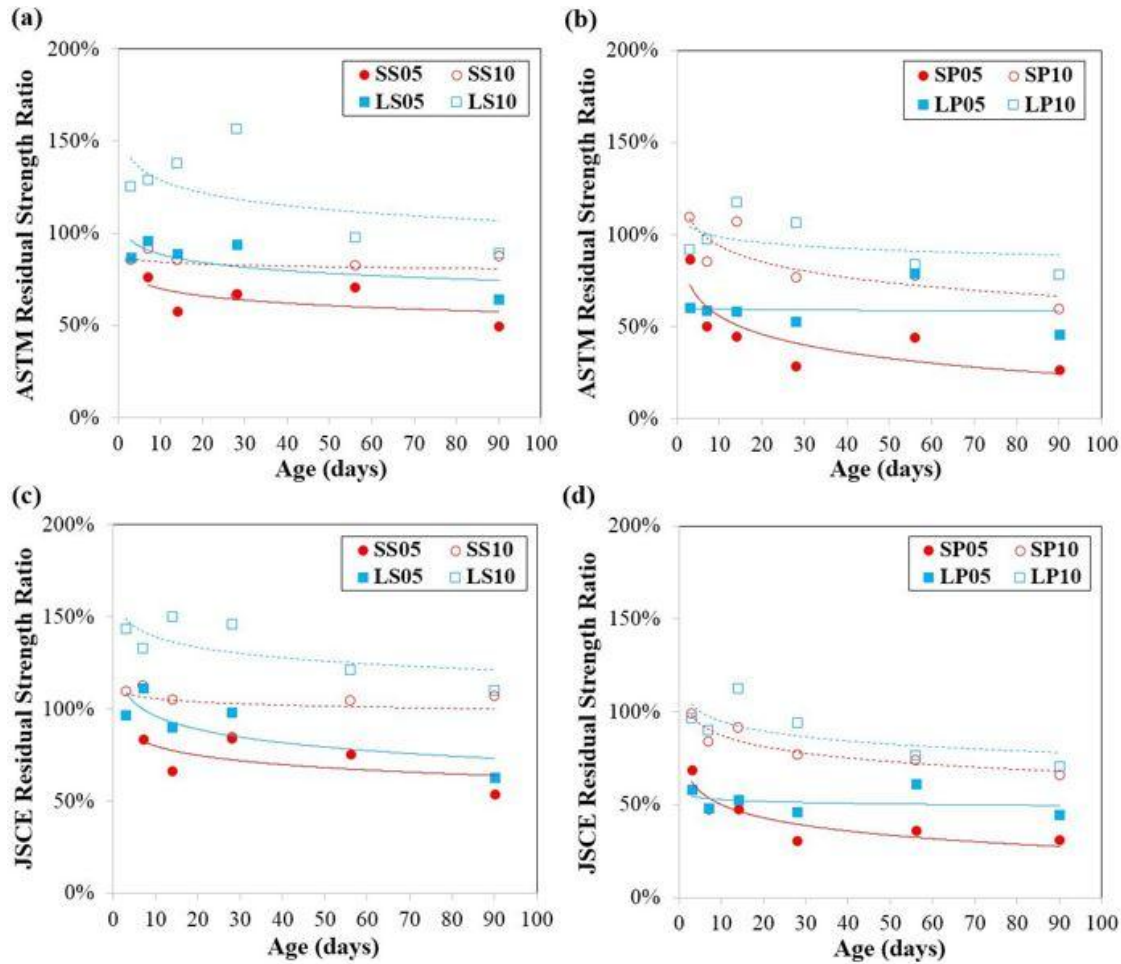


Figure 3.10 Residual strength ratio versus age, (a) and (c) for SFRC and (b) and (d) for PFRC

Since different fiber types, dosages, and volume fractions were measured, observations based on these differences relative to the ASTM residual strength were presented in Figure 3.8. All FRCs showed an increased R_{150} as the fiber length or volume fraction increased, as represented specifically in Figure 3.8 (a), (c), and (d). The FRCs with higher aspect ratios were found to have a decreased residual strength ratio, as shown in Figure 3.8(b). These results are all expected based on past literature.

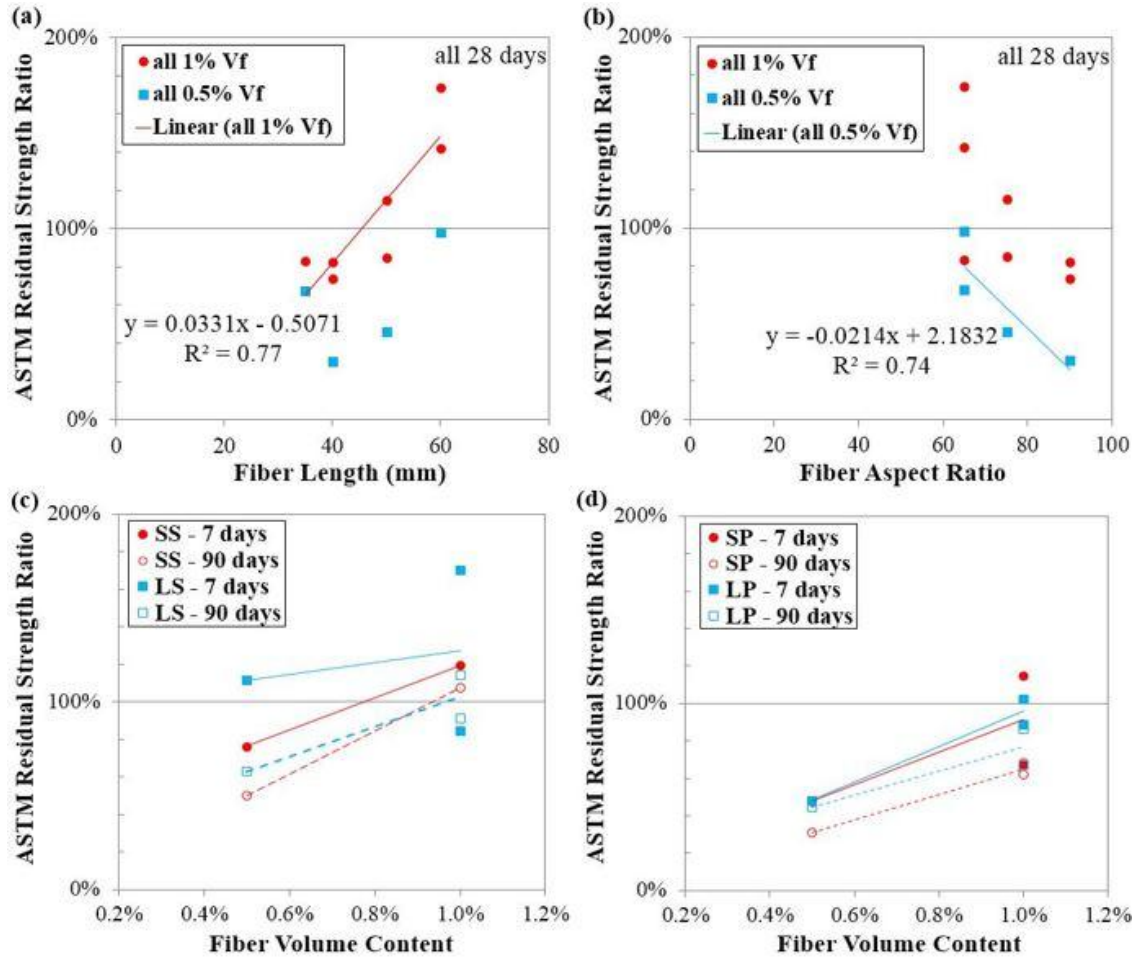


Figure 3.11 Effects of fiber length, aspect ratio, volume fraction, and material type on ASTM residual strength ratio

3.6 Fracture Energy

Table 3.5 shows the age-dependent changes in fracture energy for both plain concrete and FRCs. Figure 3.9 illustrates the effect of fiber on cut-off fracture energy, $G_{FRC, 2.5mm}$, while the total fracture energy, G_F , of plain concrete was included for comparison purposes. The wedge-splitting tensile method is different than the ASTM C1609 method because it provides a more stable controlled reading after the peak load has been reached. The energy values of this fracture test method are also expected to also be different than a flexural test because of the different geometry and displacement measurement location on the specimens. It can be seen that the fracture energy for all FRC samples clearly increased with age. The trend of increasing fracture energy with age is in good agreement with findings by other researchers (Hodicky et al. 2013). Longer fibers, either steel or polypropylene, had a greater increase in fracture energy with age, compared with shorter fibers. The increased fracture energy versus age seen with the shorter polypropylene fiber may be unexpected since the residual strength in Figure 3.6(b) was found to decrease; however, other research studies have also reported a possible decrease in the fracture energy with age for this same fiber type (Bordelon 2007). Again, some discrepancy between fracture energy and residual strength trends may be due to the difference in test methods, where residual strength methods indicate an averaged flexural performance across any multiple cracking location, and fracture methods specifically monitor a single crack growth.

Table 3.7 Averaged Wedge Splitting Fracture Energy of Plain and FRC Specimens

Specimen	Age (days)	7	28	90
Plain	G_F (N/m)	81.3	87.56	106.89
SS05	$G_{FRC, 2.5mm}$ (N/m)	728.02	750.74	1324.6
SS10	$G_{FRC, 2.5mm}$ (N/m)	955.06	1046.32	1620.9
LS05	$G_{FRC, 2.5mm}$ (N/m)	424.69	1141.51	2137
LS10	$G_{FRC, 2.5mm}$ (N/m)	1051.04	1749.04	2739.5
SP05	$G_{FRC, 2.5mm}$ (N/m)	489.73	511.79	648.39
SP10	$G_{FRC, 2.5mm}$ (N/m)	531.18	510.06	716.57
LP05	$G_{FRC, 2.5mm}$ (N/m)	525.43	688.98	821.11
LP10	$G_{FRC, 2.5mm}$ (N/m)	703.43	990.67	901.39

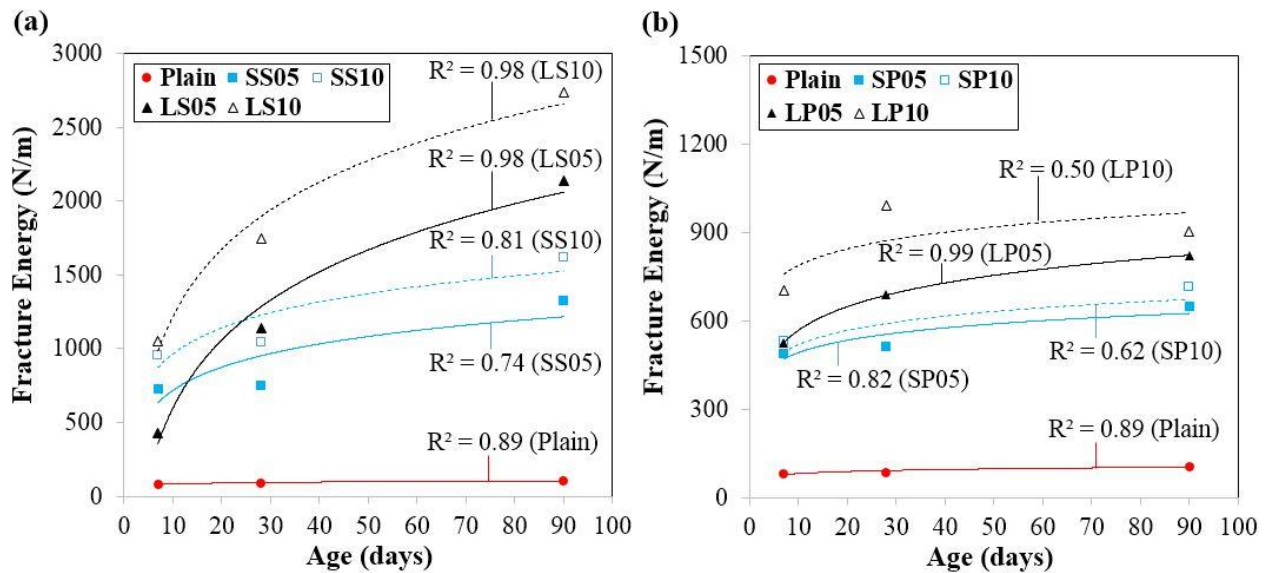


Figure 3.12 Fracture energy versus age for (a): SFRC and (b): PFRC

4. CONCLUSIONS

This study aimed to investigate the age-dependent changes in flexural and fracture properties of FRC. A total of four different macro-fiber types with three different volume contents (0%, 0.5%, and 1.0%) were selected for this study. The four fiber types studied included a short steel hooked (SS), long steel hooked (LS), short smooth polypropylene (SP), and long embossed polypropylene (LP) fibers. Most tests had two or three replicates per age and per fiber type. Statistical p-values were calculated comparing FRC with plain concrete at the same ages, and trend line goodness of fit R^2 values were calculated.

The present study indicated that the compressive strength, free drying shrinkage, coefficient of thermal expansion, and modulus of rupture statistically had negligible effects regardless of the addition of these macro-fibers to the concrete. Deflection-hardening flexural responses were only seen in steel fibers and sometimes only with higher fiber contents. The post-cracking residual strength of these deflection-hardening FRCs was found to increase with age. The deflection-softening FRCs had high variability and low R^2 values in the trends observed for residual strengths. Still, from general observations, the long PFRC samples showed an increased residual strength with age, while the short PFRC samples showed the decreased residual strength versus age.

All FRCs were observed to have a potential decreased residual strength ratio with age, as predicted due to the increase in modulus of rupture with age. All FRCs showed the expected increased fracture energy versus age, with SFRCs exhibiting higher fracture energies compared with that of PFRCs. The variability was found to be high among the flexural test properties, therefore these age-dependent trends, specifically with respect to residual strength, may need to be verified by future studies with a larger number of replicates. Based on the probable test age-dependence observed in the residual strength ratio, the age of the flexure property need to be specified in order to reduce this uncertainty in the design of FRC overlays.

5. REFERENCES

- Altoubat, S. A., Roesler, J. R., Lange, D. A., and Rieder, K.-A. (2008). "Simplified method for concrete pavement design with discrete structural fibers." *Construction and Building Materials*, 22(3), 384–393.
- American Association of State Highway and Transportation Officials. (2011). AASHTO T336, Standard Test Method for the Coefficient of Thermal Expansion of Hydraulic Cement Concrete.
- ASTM C157. (2008). Standard Test Method for Length Change of Hardened Hydraulic-Cement Mortar and Concrete. ASTM Book of Standards Volume 04.02: Construction, ASTM International, West Conshohocken, PA.
- ASTM C1609. (2010). 1609/C 1609M-10 Standard Test Method for Flexural Performance of Fibre-Reinforced Concrete (Using Beam with Three Point Loading).
- ASTM C39. (2005). Standard Test Method for Compressive Strength of Cylindrical Concrete Specimens. ASTM Book of Standards Volume 04.02: Construction, ASTM International, West Conshohocken, PA.
- Banthia, N., and Sheng, J. (1996). "Fracture toughness of micro-fiber reinforced cement composites." *Cement and Concrete Composites*, 18(4 SPEC. IS), 251–269.
- Bayasi, Z., and Zeng, J. (1993). "Properties of polypropylene fiber reinforced concrete." *ACI Materials Journal*, 90(6), 605–610.
- Bernard, E. S. (2015). "Age-dependent changes in post-crack performance of fibre reinforced shotcrete linings." *Tunneling and Underground Space Technology*, Elsevier Ltd, 49, 241–248.
- Bolat, H., Şimşek, O., Çullu, M., Durmuş, G., and Can, Ö. (2014). "The effects of macro synthetic fiber reinforcement use on physical and mechanical properties of concrete." *Composites Part B: Engineering*, 61, 191–198.
- Bordelon, A. C. (2007). "Fracture Behavior of Concrete Materials for Rigid Pavement Systems." (J. R. Roesler, ed.), University of Illinois at Urbana-Champaign, Urbana, IL.
- British Standards Institute. (2005). BS EN 14651:2005 + A1:2007, Test method for metallic fibre concrete - measuring the flexural tensile strength (Limit of Proportionality (LOP) residual).
- Brühwiler, E., and Wittmann, F. H. (1990). "The wedge splitting test, a new method of performing stable fracture mechanics tests." *Engineering Fracture Mechanics*, 35(1–3), 117–125.
- Buch, N., Jahangirnejad, S., and Kravchenko, S. (2008). "Laboratory investigation of effects of aggregate geology and sample age on coefficient of thermal expansion of portland cement concrete." *Transportation Research Board 87th Annual Meeting*.
- Campione, G. (2006). "Influence of FRP wrapping techniques on the compressive behavior of concrete prisms." *Cement and Concrete Composites*, 28(5), 497–505.
- Carlswärd, J. (2006). "Shrinkage cracking of steel fibre reinforced self-compacting concrete overlays: test methods and theoretical modelling." Lulea University of Technology, Lulea, Sweden.

- Chan, Y.-W., and Li, V. C. (1997). "Age effect on the characteristics of fibre/cement interfacial properties." *Journal of Materials Science*, 32(19), 5287–5292.
- Chanh, N. (2004). "Steel fiber reinforced concrete." Faculty of Civil Engineering Ho Chi Min City University of Technology, 108–116.
- Chanvillard, G., Aitcin, P.-C., and Lupien, C. (1989). "Field evaluation of steel fiber reinforced concrete overlay with various bonding mechanisms." *Transportation Research Record*, (1226), 48–56.
- Fraternali, F., Ciancia, V., Chechile, R., Rizzano, G., Feo, L., and Incarnato, L. (2011). "Experimental study of the thermo-mechanical properties of recycled PET fiber-reinforced concrete." *Composite Structures*, 93(9), 2368–2374.
- Gopalaratnam, V. S., Shah, S. P., Batson, G., Criswell, M., Ramakishnan, V., and Mecharatana, M. (1991). "Fracture Toughness of Fiber Reinforced Concrete." *ACI Materials Journal*, 88(4), 339–353.
- Grzybowski, M., and Shah, S. P. (1990). "Shrinkage cracking of fiber reinforced concrete." *ACI Materials Journal*, 87(2), 138–148.
- Hodicky, K., Hulin, T., Schmidt, J. W., and Stang, H. (2013). "Wedge splitting test on fracture behaviour of fiber reinforced and regular high performance concretes." *13th International Conference on Fracture 2013, ICF 2013*, 634–643.
- Hoff, G. (1987). "Durability of fiber reinforced concrete in a severe marine environment." *Concrete Durability - Katharine and Bryant Mather International Conference SP-100*, American Concrete Institute, 997–1041.
- Hsie, M., Tu, C., and Song, P. S. (2008). "Mechanical properties of polypropylene hybrid fiber-reinforced concrete." *Materials Science and Engineering A*, 494(1–2), 153–157.
- Japan Society of Civil Engineers. (1984). "JSCE-SF4 Methods of tests for flexural strength and flexural toughness of steel fibre reinforced concrete." *Concrete Library International*, Part III-2(3), 58–61.
- Jenq, Y. S., and Shah, S. P. (1986). "Crack propagation in fiber-reinforced concrete." *Journal of Structural Engineering (United States)*, 112(1), 19–34.
- Kim, D. J., Naaman, A. E., and El-Tawil, S. (2008). "Comparative flexural behavior of four fiber reinforced cementitious composites." *Cement and Concrete Composites*, 30(10), 917–928.
- Kim, M. O., and Bordelon, A. (2015). "Determination of total fracture energy for fiber-reinforced concrete." *American Concrete Institute, ACI Special Publication*.
- Kim, M. O., and Bordelon, A. (2016). Fiber effect on interfacial bond between concrete and fiber-reinforced mortar. *Transportation Research Record*.
- Koo, B.-M., Kim, J.-H. J., Kim, S.-B., and Mun, S. (2014). "Material and Structural performance evaluations of Hwangtoh admixtures and recycled PET fiber-added eco-friendly concrete for CO₂ emission reduction." *Materials*, 7(8), 5959–5981.

- Krstulovic-Opara, N., Haghayeghi, A. R., Haidar, M., and Krauss, P. D. (1995). "Use of conventional and high-performance steel-fiber reinforced concrete for bridge deck overlays." *ACI Materials Journal*, 92(6), 669–677.
- Lu, X., Lu, X., Guan, H., and Ye, L. (2013). "Collapse simulation of reinforced concrete high-rise building induced by extreme earthquakes." *Earthquake Engineering and Structural Dynamics*, 42(5), 705–723.
- Malmberg, B., and Skarendhal, A. (1978). "Method of studying the cracking of fiber concrete under restrained shrinkage." *RILEM Symposium on Testing and Test Methods of Fiber Cement Composites*, 173–179.
- Mangat, P. S., and Gurusamy, K. (1987). "Chloride diffusion in steel fibre reinforced marine concrete." *Cement and Concrete Research*, 17(3), 385–396.
- Meddah, M. S., and Bencheikh, M. (2009). "Properties of concrete reinforced with different kinds of industrial waste fibre materials." *Construction and Building Materials*, 23(10), 3196–3205.
- Mobasher, B., Bakhshi, M., and Barsby, C. (2014). "Backcalculation of residual tensile strength of regular and high performance fiber reinforced concrete from flexural tests." *Construction and Building Materials*, 70, 243–253.
- Naaman, A. E., and Reinhardt, H. W. (2006). "Proposed classification of HPFRC composites based on their tensile response." *Materials and Structures/Materiaux et Constructions*, 39(289), 547–555.
- Ochi, T., Okubo, S., and Fukui, K. (2007). "Development of recycled PET fiber and its application as concrete-reinforcing fiber." *Cement and Concrete Composites*, 29(6), 448–455.
- Pereira De Oliveira, L. A., and Castro-Gomes, J. P. (2011). "Physical and mechanical behaviour of recycled PET fibre reinforced mortar." *Construction and Building Materials*, 25(4), 1712–1717.
- RILEM TC 162-TDF. (2003). "RILEM TC 162-TDF: Test and design methods for steel fibre reinforced concrete. Sigma-epsilon design method. Final Recommendation." *Materials and Structures*, 36, 560–567.
- Shin, H.-C., and Chung, Y. (2011). "Determination of Coefficient of Thermal Expansion Effects on Louisiana's PCC Pavement Design." *Louisiana Transportation Research Center*.
- Soliman, A. M., and Nehdi, M. L. (2014). "Effects of shrinkage reducing admixture and wollastonite microfiber on early-age behavior of ultra-high performance concrete." *Cement and Concrete Composites*, 46, 81–89.
- Song, P. S., Hwang, S., and Sheu, B. C. (2005). "Strength properties of nylon- and polypropylene-fiber-reinforced concretes." *Cement and Concrete Research*, 35(8), 1546–1550.
- Wang, Y., Li, V. C., and Backer, S. (1990). "Experimental determination to tensile behavior of fiber reinforced concrete." *ACI Materials Journal*, 87(5), 461–468.
- Ward, R. J., and Li, V. C. (1990). "Dependence of flexural behavior of fiber reinforced mortar on material fracture resistance and beam size." *ACI Materials Journal*, 87(6), 627–637.

Won, M. (2005). Improvements of testing procedures for concrete coefficient of thermal expansion. Transportation Research Record.

Zhang, J., and Li, V. C. (2001). "Influences of fibers on drying shrinkage of fiber-reinforced cementitious composite." *Journal of Engineering Mechanics*, 127(1), 37–57.